ARCHIVES OF ELECTRICAL ENGINEERING VOL. 62(3), pp. 463-472 (2013)

DOI 10.2478/aee-2013-0037

High voltage pulse generation using magnetic pulse compression*

MICHAŁ BALCERAK, MARCIN HOŁUB, RYSZARD PAŁKA

Electrical Engineering Department
West Pomeranian University of Technology Szczecin
Sikorskiego 37, 70-313 Szczecin, Poland
tel. (48-91) 449-48-73, fax. (48-91) 449-43-17
e-mail: {mbalc/mholub/rpalka}@zut.edu.pl

(Received: 26.06.2012, revised: 12.12.2012)

Abstract: The paper presents an overview of a method of nanosecond-scale high voltage pulse generation using magnetic compression circuits. High voltage (up to 18 kV) short pulses (up to 1.4 μs) were used for Pulsed Corona Discharge generation. In addition, the control signal of parallel connection of IGBT and MOSFET power transistor influence on system losses is discussed. For a given system topology, an influence of core losses on overall pulse generator efficiency is analysed.

Key words: kicker power supply, power source for pulse corona discharge, magnetic pulse compression, parallel connection of IGBT and MOSFET transistors

1. Introduction

In order to generate microdischarge plasma or a pulsed corona discharge in barrier-less reactor systems, a high voltage pulse generator is necessary for providing nanosecond-scale pulses with amplitudes ranging from a few to tenths of kilovolts. Apart from the peak voltage value of the reactor supply voltage, the rising slope timing of the voltage and the pulse duration play an important role as well. Extremely short pulses with maximal rising slopes offer the best results in non-thermal plasma generation [1].

A unique Marx-Fitch topology based pulse generator was developed and constructed, possessing the property of small output impedance [2]. The basic structure of the proposed Kicker Power Supply (KPS) system with a magnetic pulse compressor is depicted in Figure 1. In order to achieve higher voltage amplitudes, such modules can be connected in series.

* This is extended version of a paper which was presented at the 22th *Symposium on Electromagnetic Phenomena in Nonlinear Circuits*, Pula, Croatia, 26.06-29.06 2012.

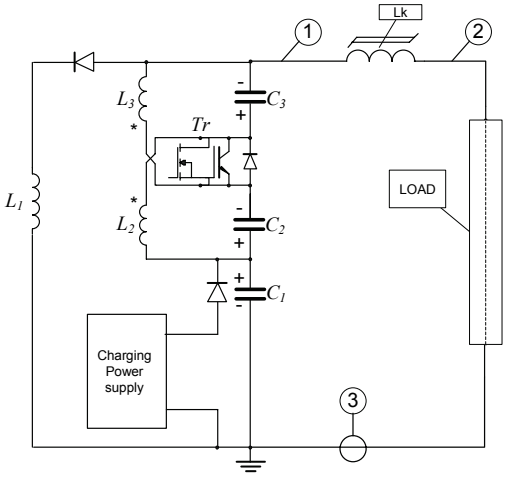

Fig. 1. Topology of a single module of the proposed pulse generator with a magnetic pulse compressor and a plasma reactor as load

The output voltage waveform can be described using the following formula [2]:

$$V_{KPS}(t) = n \cdot V_{\text{init}}(1 - 2\cos\omega t), \tag{1}$$

where: n – a number of serially connected KPS modules; V_{init} – C_1, C_2 and C_3 initial voltage; U_{KPS} – KPS output voltage; ω – angular frequency of a LC resonant circuit if $C = C_2 = C_3$ and $L = L_2 = L_3$ while $\omega = 1/\sqrt{(LC)}$.

Equation (1) was obtained for the case of the pulse generator's idle operation, because the output voltage peak value decreases as the plasma reactor increases the amount of consumed charge.

2. Magnetic pulse current compression

Through the use of magnetic pulse compression, it is possible to achieve higher voltage pulse steepness and higher maximal values of reactor currents. A typical two-stage, magnetic pulse compressor system topology is depicted in Figure 2a. Voltage and current waveforms of respective compressor stages is given in Figure 2b.

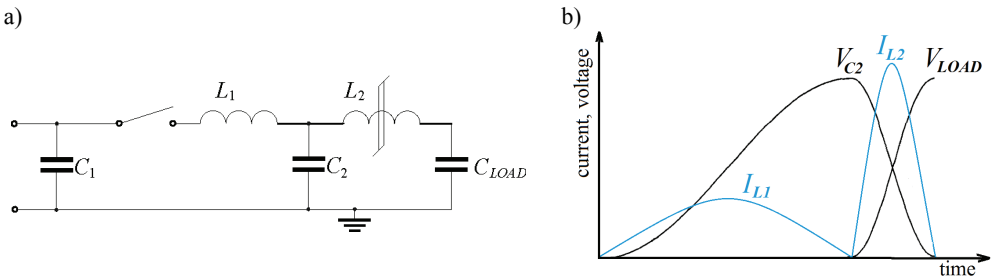

Fig. 2. Typical topology (a) and voltage and current waveforms of respective compressor stages of a magnetic pulse compressor (b) (L2 and L3 are magnetic, saturable inductors), based on [3]

Magnetic switches are robust and can also be used for high repetition rates (several kHz), however, their energy conversion efficiency for short pulse generation is relatively low (typically 60-80%) [4]. The shape of the magnetization curve is unfortunately negatively affected while decreasing the magnetization pulse length, which leads to increased core losses and the quality of pulse compression further decreases. As shown in [5], magnetic core losses (FINEMET core, K101, Liyuan Metal Corp., China) can achieve six times higher values for short magnetization pulses (0.5 μs) than for longer magnetization pulses (4.5 μs).

Because of the magnetic material losses that increase with the use of higher frequencies and core saturation levels (as discussed in [6]) it was decided to use a single stage current compression circuit. For the construction of magnetic pulse compressor cores, the CMD5005 material was used. Such material is characterized by small magnetic hysteresis area even in the case of higher frequencies, which is very important in applications where a single pulse can only provide a small amount of energy to reactor electrodes.

In order to achieve the magnetic compression phenomenon, it is necessary to obtain a magnetic flux density that highly exceeds the saturation value of BSAT for a given core construction and material. The value of magnetic flux density B can be obtained using a well known formula:

$$\int V(t)dt = \Delta B \cdot S_{Fe} \cdot z, \tag{2}$$

where $V(t)$ is the used voltage, ΔB is the magnetic flux density, z is the number of turns, S_{Fe} is the core cross-section area.

According to Equation (2), in order to reduce the necessary magnetic compressor core cross-section the number of turns z can be increased (which leads to increased parasitic inductance of the compressor), an additional demagnetisation circuit can be used in order to increase the ΔB (Magnetic Recovery Circuit, [7]), or the voltage pulse shape can be influenced in order to minimize its time domain integral value. Figure 3 gives an illustrative representation of exemplary core sizes for identical pulse lengths and amplitudes (produced after [8]). As can be noted, the minimal possible core cross section can be obtained using the Magnetic Recovery circuitry, but it must be noted that the demagnetisation circuit has to possess large inductance, that in addition will be proper for voltage values induced during demagnetisation and high current amplitudes [7].

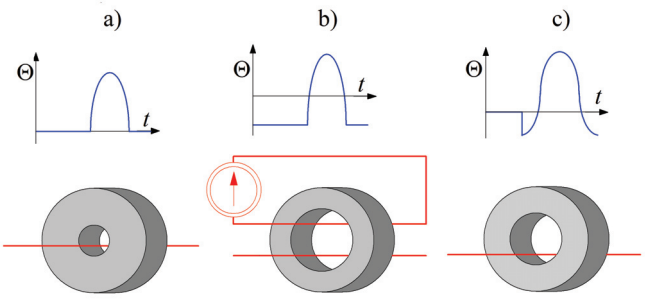

Fig. 3. Illustrative representation of magnetic flux densities and core sizes necessary for magnetic pulse compression circuits: a) unipolar pulse operation, b) unipolar pulse operation with the Magnetic Recovery Circuit, c) bipolar pulse shapes as proposed in this work

As can be noticed, it is possible to reduce the necessary core size using proper pulse shapes without the need for Magnetic Recovery Circuit implementation. The proposed pulse generator topology exhibits this property (Fig. 4), which leads to a reduction of necessary magnetic compressor core cross-section of 33% when compared to a unipolar waveform of the same voltage peak value and identical period. This reduction rate can be expressed using the analytical approach given in Equation (3).

$$\frac{\int_0^{T/2} V_{init}\left(1-2\cos\omega_0 t\right)dt}{\int_0^{T/2} 1.5\,V_{init}\left(1-\cos\omega_0 t\right)dt} = \frac{\pi\sqrt{LC}\cdot V_{init}}{1{,}5\pi\sqrt{LC}\cdot V_{init}} \approx 0{,}67. \tag{3}$$

Results of time domain analysis of both voltage shapes and resulting time integral value is depicted in Figure 4.

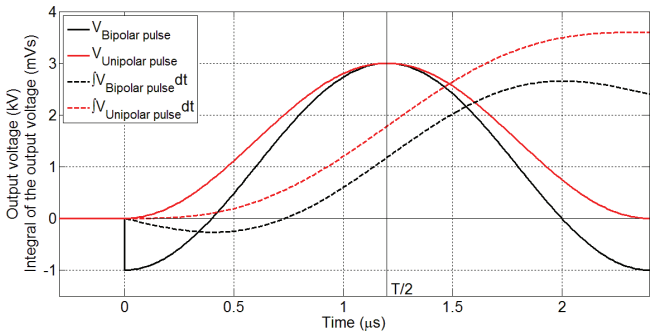

Fig. 4. A comparison of unipolar and partially bipolar (KPS) voltage waveforms and their time integrals

3. Current compression simulation results

In the modelling phase 10 magnetic cores T1113 made of CMD5005 material were simulated using the datasheet *B-H* curve. A non-linear inductance was constructed in the Simplorer

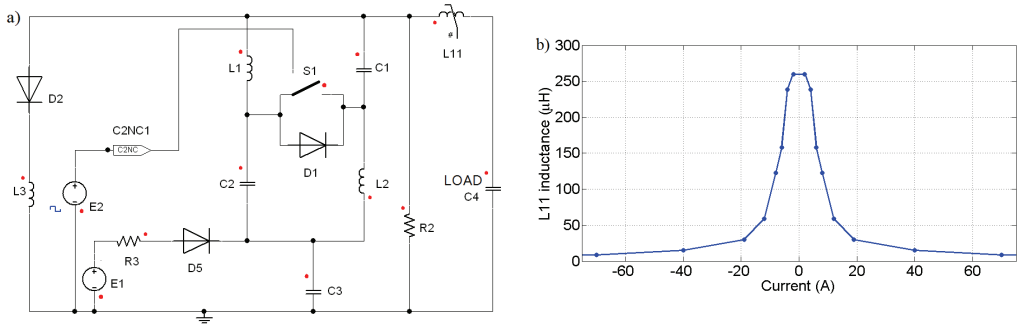

Fig. 5. a) Simulation model created in Simulink 7.0 environment and b) Current – inductance value characteristics $L = f(I)$ for L11 (saturable compressor core) created for the purpose of non-linear modelling, based on T1113 – CMD5005 datasheet for 3 wires on 10 cores

7.0 simulation environment. The inductance value – current characteristics of such a set-up is presented in Figure 5b, the simulation model is given in Figure 5a.

An exemplary set of theoretical waveforms, including voltage before and after compression and compressor current, are depicted in Figure 6. A successful use of a single stage compressor is obtained.

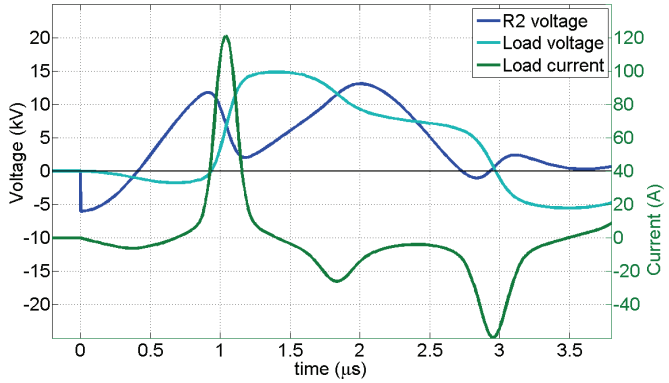

Fig. 6. Simulated compressor waveforms

As can be noticed, magnetic compression is achieved during two points of operation: the rising and the falling slope of the output voltage.

4. Current compression experimental investigations and efficiency optimisation

In order to investigate the practical properties of the pulse generation set-up, a set of prototypes were constructed. Basic experiments were led using an experimental pulse generator construction based on a topology depicted in Figure 1. The experimental construction consists of 10 such modules connected serially, supplied with an initial voltage value of V_{init} = 600 V each. Capacitors were implemented using fast, polypropylene, high voltage type WIMA FKP1 with the value of $C_1 = C_2 = C_3 = 44$ nF each. Resonant inductor inductance value was $L_2 = L_3 = 4.3$ µH. Considering a lumped pulse generator schematic construction as in Fig. 1, this would be equivalent to $C_1 = C_2 = C_3 = 4.4$ nF (ten modules in series) $L_2 = L_3 = 43$ µH and the overall initial voltage of $V_{\text{init}} = 6$ kV. Generator construction is depicted in Figure 7.

All the electrical waveforms were recorded using Tektronix DPO4054 (500 MHz, 2.5 GS/s). Voltage before and after pulse magnetic compression was measured by Tektronix High-Voltage probe (type P6015 A, 20 kV_{DC}, 75 MHz, 3.0 pF, 100 MΩ) and LeCroy High-Voltage probe (type PMK-14KVAC). Current was measured by a Pearson current monitor (model 6585, 250 MHz).

An additional set of experiments was led in order to evaluate the efficiency and voltage rising slope properties for different magnetic compressor parameters. Two different load capacitances were chosen, namely: C_{load} = 1.5 nF, which is equal to the output capacity of con-

verter (KPS) and C_{load2} = 0.73 nF, which is equal to half of the output capacity of converter (KPS). Measurement results are summarized in Table 1. As can be noticed, increasing the steepness ratio and the energy delivered to the load decrease the efficiency. Increasing load capacitance also has a fundamental impact on the overall efficiency.

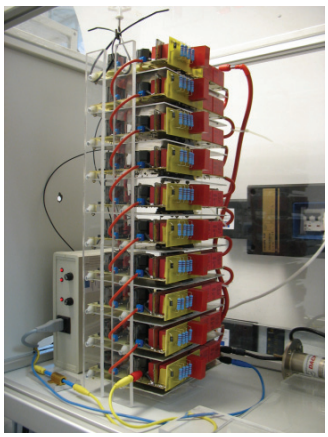

Fig. 7. Experimental, 10-stage KPS generator construction

Table 1. Summary of measurement results for different compressor parameters and load capacitances. In each cease the compressor core was constructed using a setup of 10 pieces of T1113-CMD5005

No. of compressor turns	**$^{dV}/_{dt}$ before compression (V/ns)**	**$^{dV}/_{dt}$ after compression (V/ns)**	**Steepness ratio**	**Load energy (mJ)**	**Efficiency η (%)**
$C_{Load} = C_{KPS}$ = 1.5 nF					
1	22.3	29	1.3	102.2	77
2	29.1	54.4	1.87	102.8	69
3	34	66.1	1.94	144.2	76
$C_{Load2} = 1/2C_{KPS}$ = 0.73 nF					
1	22.7	29.4	1.3	76.6	81
2	29.9	60.5	2.03	73.4	67
3	29.5	80.9	2.74	113.9	70

The given efficiency was evaluated on the basis of energy balance of the input capacitors and the inductor power loss. This was measured using the time integral of the inductor, half-period voltage and current product. The resulting efficiency was calculated using Equation (4).

$$\eta = \frac{\frac{V_{init}^2 (C_1 + C_2 + C_3)}{2} - \int_0^{T/2} v_{Lk} i_{Lk} dt}{\frac{V_{init}^2 (C_1 + C_2 + C_3)}{2}} \cdot 100, \tag{4}$$

where: V_{init} = 6 kV – initial capacitor voltage of parallel connection of C_1, C_2 i C_3, C_{KPS} = 4.4 nF.

In order to verify the simulated model, the output current compression was examined. Experiment parameters: C_{Load} = 1.5 nF, 3 turns on 10 cores of T1113-CMD5005 material, C_1 = C_2 = C_3 = 4.4 nF, L_1 = L_2 = 43 µH, R_2 = 100 MΩ, V_{init} = 6 kV, C_4 = 1.5 nF) including voltage before and after compression and compressor current are depicted in Figure 8. A successful use of a single stage compressor is obtained.

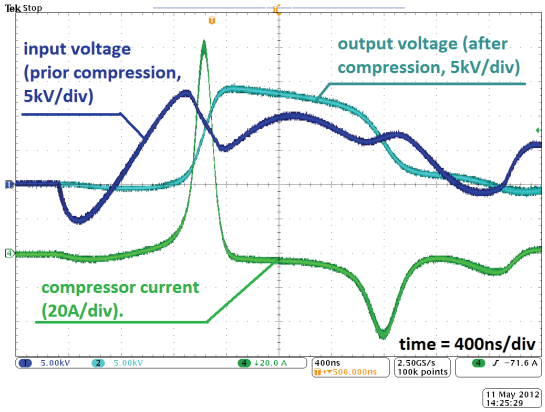

Fig. 8. Exemplary compressor operation waveforms: input voltage (prior compression, dark blue, 5 kV/div) output voltage (after compression, bright blue, 5 kV/div), compressor current (green, 20 A/div)

As can be noticed in comparison to Figure 8, magnetic compression is achieved during two points of operation: the rising and the falling slope of the output voltage. Small differences between simulated and experimental waveforms can be explained by the simplified magnetic circuit model in the simulator, neglecting the hysteretic loop and therefore also losses in the magnetic circuit. Losses in other active and passive components are also neglected in the simulation model.

Because of the extended lifetime, power electronic solid state switches were used in the form of IGBT and MOSFET transistors [4]. In order to generate high voltage, high power pulses on the input of the magnetic pulse compressor, it is necessary to use fast semiconductors with maximum blocking voltages and conduction currents. Therefore, it was decided that a parallel pair of both MOSFET (STW20NB50) and IGBT (IRG4PC50FD) be used, resulting in a compensation effect of the nonlinear switching-on characteristics of the power IGBT with the nonlinear on-state MOSFET characteristics [9]. At the same time, each magnetic compressor stage lowers the overall pulse generator efficiency [10]. In order to avoid a large number of stages, the shortest possible pulses have to be generated at the compressor input. An additional model of a Kicker Power Supply was constructed in order to generate 300 ns pulses. It is a construction including only one module. A simplified construction of the examined topology is given in Figure 9.

In order to minimize the pulse duration, capacitance was reduced to C_1 = C_2 = C_3 = 3.3 nF and inductances L_1 = L_2 = 1 µH. Simultaneously the overall pulse energy was also reduced. In order to maximize the pulse generation efficiency, transistor losses were carefully examined.

MOSFET power transistors are usually characterized with higher allowable di/dt ratings during switching-on, while IGBT transistors generally have higher current ratings during conduction. This is visually explained in Figure 10. Using both technologies in a parallel connection allows to combine those benefits in a single set-up.

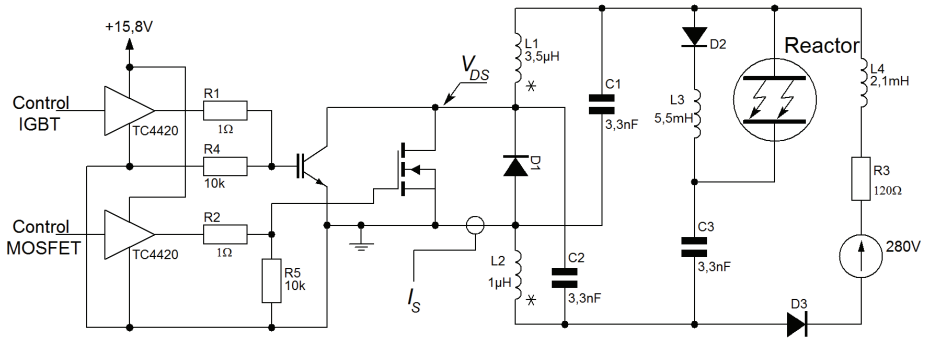

Fig. 9. Pulse generator transistor losses measurement setup

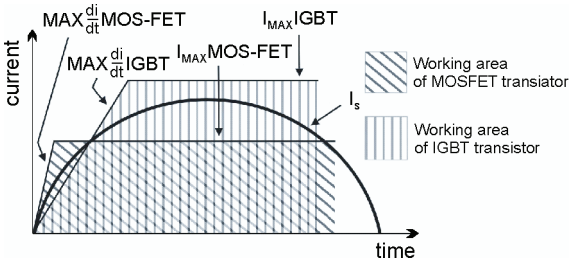

Fig. 10. Schematical description of the nonlinearity compensation effect of a IGBT – MOSFET pair

Using a parallel connection of both switch technologies, loss reduction was achieved. Both transistors in parallel were characterized by a 65% overall loss reduction, compared to a single IGBT switch and 57% loss reduction compared to a single MOSFET switch. Measurements were led for the supply voltage of 250 V DC. Switching the IGBT transistor earlier than the MOSFET switches leads to minimized switch-on losses, as shown in Figure 11.

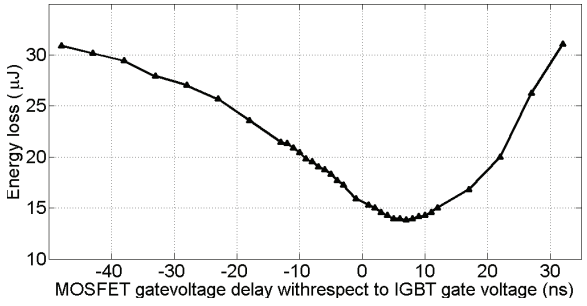

Fig. 11. Energy loss of both transistors in single output pulse as a function of MOSFET gate voltage delay with respect to IGBT gate voltage

Transistor energy loss was measured as a time integral of transistor voltage and current product over a single LC circuit recharge. Current measurement points are depicted in Figure 9. The single recharge energy loss was respectively 39.32 μJ for IGBT transistor recharge, 32.12 μJ for MOSFTE transistor recharge, 15.01 μJ in case of parallel IGBT-MOSFET operation and 13.81 μJ in case of parallel operation with optimized switching times. In case of optimal timing, the MOSFET gate control signal was delayed with respect to IGBT gate control at 7 ns.

Due to the described control system, overall, high optimisation generator efficiency was obtained in the case of nanosecond pulse generation. Such pulses can be directly used for pulsed plasma reactor supply or as an input for magnetic pulse compressors. It is important to notice that such generator set-up allows for short pulse generation without the use of multi-stage magnetic compressors.

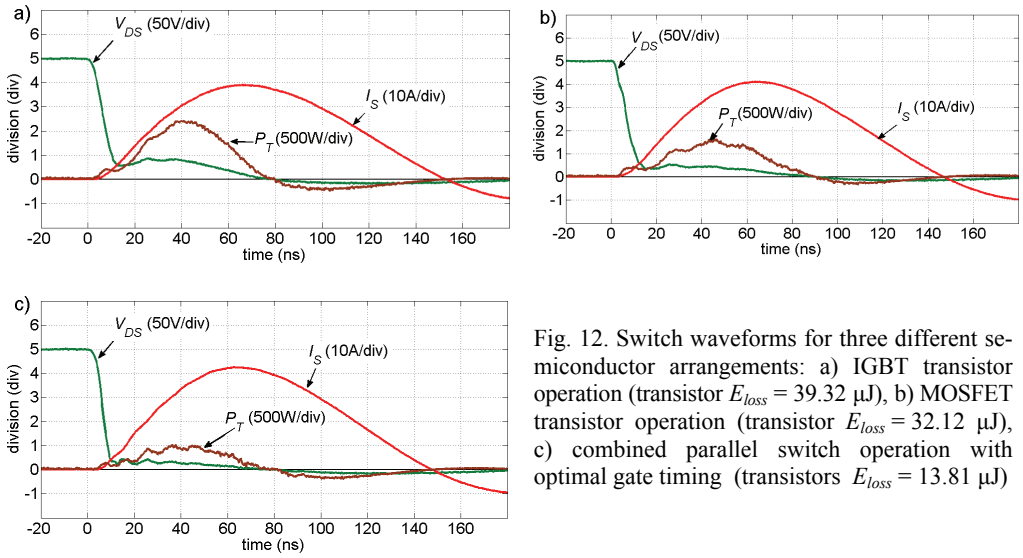

Fig. 12. Switch waveforms for three different semiconductor arrangements: a) IGBT transistor operation (transistor E_{loss} = 39.32 µJ), b) MOSFET transistor operation (transistor E_{loss} = 32.12 µJ), c) combined parallel switch operation with optimal gate timing (transistors E_{loss} = 13.81 µJ)

Figure 12 gives an overview of measured transistor waveforms (switch voltage V_{DS}, current I_S and resulting loss power P_T) for 3 different arrangements: a) IGBT transistor operation, b) MOSFET transistor operation, c) combined parallel switch operation with optimal gate timing. The partly negative momentary power value is due to switch parasitic inductances.

5. Summary

An efficient generator set-up is presented, allowing for output voltage multiplication and solid state switch-based construction. Its unique properties also include the necessary pulse compressor magnetic core cross section reduction rate of 33%. An IGBT – MOSFET power switch parallel connection was used improving the overall pulse generator efficiency.

Magnetic pulse compression allows for an increased output voltage rising slope steepness in the case of high voltage nanosecond-scale pulse generator set-ups. Higher reactor currents and steeper electrode voltages improve the non-thermal pulsed type plasma generation. After using the magnetic pulse compressor, it was possible to obtain stable, non-thermal, pulsed plasma generation in a corona type reactor. Magnetic material losses play an important role in the overall generator efficiency and have to be analysed with utmost attention.

References

[1] Wang D., Namihira T., Akiyama H., *Pulsed Discharge Plasma for Pollution Control.* [In:] Villanyi V. (Ed.). *Air Pollution.* Sciyo, Rijeka, Croatia, ISBN 978-953-307-143-5, pp. 265-287 (2010).

[2] Kalisiak S., Hołub M., *Modified Fitch generator topology for non-thermal plasma applications*. Przegląd Elektrotechniczny (Polish Electrical Review), No 7/2009, pp. 134-137 (2009).

[3] Smith C.H., *Terawatts and Nanoseconds-Metallic Glasses in Pulse Power Systems.* Journal of Materials Engineering 12(1): 35-40 (1990).

[4] Liu Z., Pemen A.J.M., van Hoppe R.T.W.J., Winands G.J.J., van Heesch E.J.M., Yan K., *An Efficient, Repetitive Nanosecond Pulsed Power Generator with Ten Synchronized Spark Gap Switches.* IEEE Transactions on Dielectrics and Electrical Insulation, August 2009, 16(4): 918-925 (2009).

[5] Zhang D.D., Yan P., Sun Y.H., Wang J., Zhou Y., Pan R.Z., *Characteristics of Magnetic Core in Magnetic Pulse Compression System.* Acta Physica Polonica A 6(115), Proceedings of the 2nd Euro-Asian Pulsed Power Conference, Vilnius, Lithuania, September 22-26 (2008).

[6] Shen W., Wang F., Boroyevich D., Tipton C. W., *Loss Characterization and Calculation of Nanocrystalline Cores for High-Frequency Magnetics Applications.* IEEE Transactions on Power Electronics, January 2008, 23(1): 475-484 (2008).

[7] Wang D., Wu W., Li D., Wang L., *Compact magnetic compression repetitive pulsed power generator based on IGBT*, International Conference on Electrical Machines and Systems ICEMS 2008, pp. 1255-1258 (2008).

[8] Utz S., Pforr J. *Turn-on behaviour of automotive multi-phase converters with coupled inductors.* 15th International Power Electronics and Motion Control Conference EPE-PEMC 2012 ECCE Europe, Novi Sad, Serbia, pp. LS3c.3-1-LS3c.3-8 (2012).

[9] Frisch M., Ernö T., *Innovative Topologies for High Efficient Solar Applications*. Power Electronics Europe, 03/2009, pp. 32-33 (2009).

[10] Jang S.D., Son Y.G., Oh J.S., Cho M.H., Koh D.J., *Pulsed Plasma Process for Flue Gas Removal from an Industrial Incinerator by Using a Peak 200-kV, 10-kA Pulse Modulator*. Journal of the Korean Physical Society, May 2004, 44(5): 1157-1162 (2004).